Wear 376-377 (2017) 1885–1891

Contents lists available at ScienceDirect

Wear

journal homepage: www.elsevier.com/locate/wear

Wear state identification using dynamic features of wear debris for on-line purpose

Yeping Peng [a,b], Tonghai Wu [a,*], Shuo Wang [a], Zhongxiao Peng [c]

[a] Key Laboratory of Education Ministry for Modern Design and Rotor-Bearing System, School of Mechanical Engineering, Xian Jiaotong University, Xian 710049, China

[b] College of Mechatronics and Control Engineering, Shenzhen University, Shenzhen 518060, China

[c] School of Mechanical and Manufacturing Engineering, The University of New South Wales, Sydney, NSW 2052, Australia

ARTICLE INFO

Article history:
Received 29 August 2016
Received in revised form
30 December 2016
Accepted 3 January 2017

Keywords:
Wear state identification
Wear mechanism analysis
Dynamic features of wear particles
On-line machine condition monitoring

ABSTRACT

Wear status identification including wear rate estimation and wear mechanism assessment can be performed using wear debris information. However, although on-line monitoring methods have distinctive advantages over off-line approaches, existing on-line monitoring methods provide limited features of wear particles and have difficulties characterising complex wear states. Most of them determine wear status based on changes in the wear rates, and the wear mechanisms are not taken into consideration. Therefore, comprehensive wear state identification is a bottleneck in real-time machine health monitoring for condition-based maintenance. In order to further advance on-line monitoring technology, this paper, in a case study format, presents a new approach for wear state characterisation using comprehensive wear debris features. For this purpose, wear experiments were carried out on a four-ball rig, and a particle imaging system was employed to capture videos of moving particles to acquire dynamic features. Based on this, wear particles were firstly counted to characterise wear rate. In this stage, a statistical clustering model was established using a mean-shift algorithm to categorise wear debris samples. A trend of wear state evolution was thus obtained. Secondly, the size, shape and colour of wear debris were extracted to identify particles into fatigue, sliding and oxides for wear mechanism analysis. The analysis results of wear mechanisms were related to the trend of the wear state. Correspondingly, a changing chart that contains the wear degree and wear mechanisms was drawn. Therefore, an on-line system has been developed to capture comprehensive particle information to assess the wear severity and mechanisms for in-depth wear analysis and full-life machine condition monitoring.

1. Introduction

Improvement of equipment reliability to prolong the lifespan of a machine is an important research topic. For tribo-systems (e.g. gearboxes and engines), wear caused by relative movements of frication parts is one of the main reasons of faults and failures [1]. Therefore, condition-based maintenance is used for fault prediction and failure prevention [2,3]. In particular, on-line wear condition monitoring has been developed and wear state identification has been used in engineering applications [4].

Visual inspection and oil analysis are two main methods for wear condition monitoring while vibration, acoustic emission, and electrostatic sensing techniques are mainly used for fault detection and diagnosis [5–7]. In particular, wear particles, which are directly produced from tribo-pairs, contain valuable wear information and are analysed for machine condition monitoring [8–10]. With the development of sensor technology and the demand of timely and comprehensive machine condition information, more and more researchers focus on real time wear state monitoring. An on-line visual ferrograph (OLVF) was employed to estimate wear conditions of a gasoline engine using wear debris concentration [11]. The OLVF is also effective to recognise the wear status of diesel engines [4]. Wu et al. combined particle concentration and dimension of equivalent circle size together to identify dynamic full-life wear states [12]. These above mentioned methods attempt to identity wear state using particle concentration and dimension. However, the extracted particle features can only reflect wear rate and wear severity. Wear mechanism analysis is challenging or impossible to be performed because, caused by magnetic forces of the OLVF, individual wear debris is difficult to be extracted from the particle chains [13].

In order to identify particle types in real time, our previous research [14] developed a dynamic particle imaging system. By utilizing this development, multi-view morphological features of

* Corresponding author.
E-mail address: wt-h@163.com (T. Wu).

http://dx.doi.org/10.1016/j.wear.2017.01.012
0043-1648/

individual particles can be extracted for in-depth wear analysis [15]. Meanwhile, on-line oxidation wear monitoring has been realised [16]. Based on this, our previous work of wear state identification in [12] is extended to comprehensively characterise wear states including wear rates and wear mechanisms using the dynamic features of on-line wear debris.

In the current work, further development is presented by analysing wear particles generated using a four-ball rig as a case study to demonstrate its capabilities. The methodology on how this approach is developed is described in Section 2. Wear tests are carried out and detailed in the same section. The dynamic particle imaging system is used to capture videos of moving wear debris generated from the tribo-balls. In Section 3, wear debris features, including quantity, size, shape and colour, are extracted from a series of image sequences for wear rate and wear mechanism analysis. Section 4 discusses the advantages of the proposed method in comparison to the existing techniques, followed by the main conclusions in Section 5.

2. Method and experiments

Wear particle characteristics, including quantity, size, shape, colour, are widely used to reveal wear conditions [17]. In particular, the amount and/or concentration of wear particles are used to determine wear rate and wear severity. The size and shape features contain the information of wear severity and wear mechanisms. The colour can indicate the wear sources, as well as oxidation wear [18]. In this work, the particles are sampled in moving conditions to image individual particles, and they are counted by utilizing video streaming for wear rate analysis. The particle quantity is as input of a mean-shift algorithm. Different wear processes are thus identified based on the clustering results. By doing this, a full-life evolution of wear states is obtained.

In order to reveal the complex wear status, shape and colour features are also extracted for wear mechanism analysis. Different to the existing method of static feature extraction [19], the current work uses the dynamic features of wear debris extracted from different views to distinguish particle types, especially fatigue and sliding particles in this paper. Furthermore, the colours of wear debris generated from steel tribo-pairs are extracted and employed to identify oxidation wear. The trend curve of wear rate and the results of wear mechanism analysis are combined together based on the sample acquisition time. As a result, the wear state identification model is developed to reveal comprehensive wear conditions including wear rate and mechanisms. Finally, the performance of the developed approach is evaluated by conducting wear tests on a full-ball rig and examining the wear tracks of the post-test balls. The experiment details are given in the following sections.

2.1. Experimental apparatus

To demonstrate that the above developed approach is able to obtain comprehensive wear particle information for on-line wear condition monitoring, experiments were carried out on a four-ball wear test rig, in which a dynamic particle imaging system was installed, as shown in Fig. 1. Particles carried in lubricating oil were transported into a flow path (see Fig. 1(a)). During this period, a CMOS was adopted to capture videos of moving particles that were sent to a computer for image processing and analysis. More details of the experimental apparatus can be found in [15].

2.2. Experimental method

The steel balls used in the experiments are made up of carbon chromium bearing steel (GCr15). The standards of the steel balls are in the hardness of HRC58-63 and the surface roughness of 0.025 mm. Accelerated experiments were carried out under the operation conditions: lubrication condition of base oil, load of 800 N and speed of 1000 revolutions per minute (rpm). To obtain a wear trend, test #1 was carried out in 5 h to generate wear debris in running-in, normal wear and severe wear condition. It needs to be mentioned here that this test was run continuously. In order to check the wear conditions of tribo-balls in different wear stages, two other tests were implemented under the same operation conditions but with different durations. Test #2 was run for 10 min to generate wear particles in a running-in state, and test #3 was operated for 2 h to reach a normal wear stage. A machine running under normal operating conditions can last for a very long time [20]. In order to obtain failure information, a destructive experiment, test #4, was carried out to simulate that a fault occurred. The shaft of the rig was manually adjusted to be eccentric, resulting in an abnormal wear process. Test #4 was run for 10 min. The key information of the four tests is summarized in Table 1.

As described in Section 2.1, the particle features were provided by the on-line image acquisition system (Fig. 1) for wear state identification. The lubrication in the oil cup was sampled and analysed every 6 min. At the first 1 min, the pumps were in the speed of 10 mL/min to flush the flow path. After that, the speed was changed to 1 mL/min and the videos were sampled for 5 min. The videos are at a rate of 50 fps (frames per second) and stored in the WMV (Windows Media Video) format.

2.3. Results of wear particle acquisition

Figure 2 shows some typical wear debris images captured in different wear stages, running-in, normal wear, and wear out, of tests #1 and #4. The size and quantity of the imaged particles vary with running time. It can be seen that wear particles spread out and well separated in the images. To get representative information statistical characteristics of wear debris were extracted. Moreover, large particles (around 50 μm) with various shapes and different colours were used to describe different wear mechanisms. Therefore, appropriate particle information was obtained for wear severity and wear mechanism analysis, of which details can be found in Section 3.

3. Comprehensive characterisation of wear status

The experimental results indicate that dynamic images of moving wear debris contain valuable wear information, which can be used to examine wear rate, wear severity and different wear mechanisms. In this section, wear severity and wear mechanism analysis are carried out based on the particle features.

3.1. Wear severity analysis

The quantity of wear particles and its change are used for wear rate assessment. In general, comparing to small particles, larger particles contain more failure information [21]. Therefore, the particles larger than 20 μm were counted. However, in the normal test (test #1), the quantity of large particles (LPQ) is small due to the narrow field of view and also because the tribo-balls were in good lubricating conditions as mentioned before. To ensure the LPQ contains representative wear information, the total wear particle quantity (TPQ) was also obtained using an imaging camera to capture wear particles whose size is greater than 5 μm. The counting results of test #1 are shown in Fig. 3.

As can be seen, the trends of TPQ and LPQ are similar. According to the reference [22], the tribo-pairs went through two stages, that is, running-in and normal wear. The running-in stage

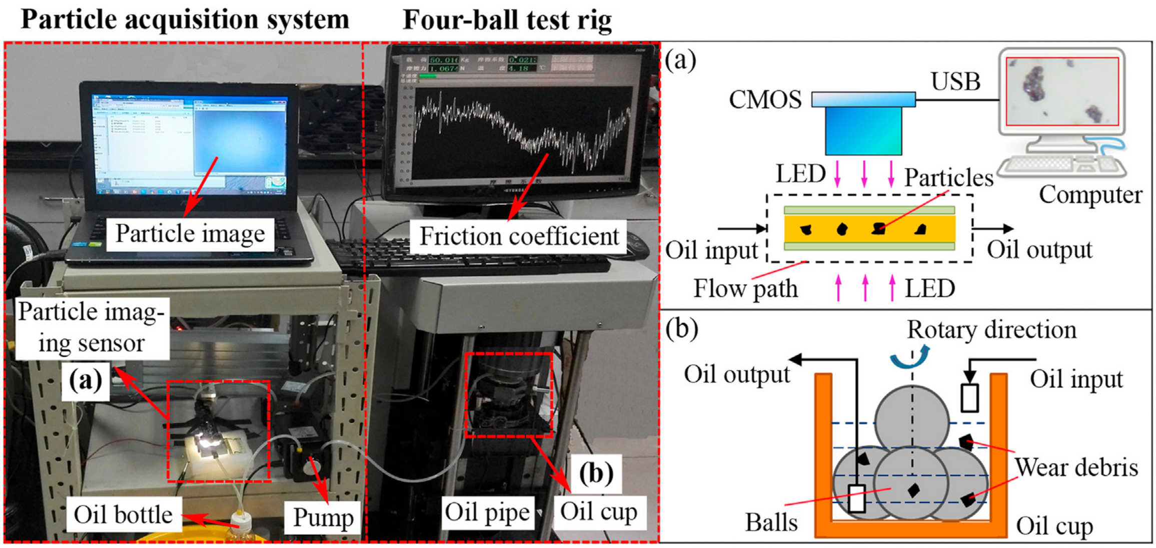

Fig. 1. Experimental set-up includes (a) principle of particle imaging sensor and (b) schematic sketch of oil cup.

Table 1
Details of the experimental process.

Test	Operation conditions	Test duration
#1	base oil, 800 N, 1000 rpm	**5 h**
#2	base oil, 800 N, 1000 rpm	**10 min**
#3	base oil, 800 N, 1000 rpm	**2 h**
#4	base oil, 800 N, 1000 rpm, **eccentric shaft**	**10 min**

was short (ended in about 10 min), followed the normal wear phase where the particle quantity increased slowly and steady due to the experimental set up. In the time interval of 200–300 min the LPQ fluctuated while the increment of the TPQ was relatively steady, indicating that the wear condition was close to severe towards the end. These results reveal that the lager particles are more sensitive to severe wear, and thus the LPQ is used to describe wear severity.

It also can be found that failure information was not captured in the normal test (test #1). Therefore, a destructive test (test #4) was carried out to obtain wear information in the abnormal wear case. The particle counting results of test #4 is listed in Table 2. Although the running time is only 10 min, both the TPQ and LPQ are significantly larger than those generated in test #1 (Fig. 3).

3.2. Wear mechanism analysis

In general, a four-ball test rig produces sliding wear debris. However, fatigue and pitting wear often occur when the machine runs in the high load and speed conditions. When the steel balls are in metal-to-metal contact, a large amount of heat is generated and oxidation wear occurs. To reveal the wear mechanisms, the shape and colour of individual wear debris were extracted to recognise particle types.

Conventional on-line monitoring systems image particles in two-dimension, making it difficult to distinguish fatigue and sliding wear debris [23–25]. This issue can be solved by viewing fatigue and sliding particles from different directions because the height to width aspect ratio (major width to thickness ratio, HWAR) between them is different. In general, sliding particles have a higher HWAR value than fatigue debris [26].

To verify fatigue wear occurred during test #1, multiple images of the same particles were captured at different views. Four typical

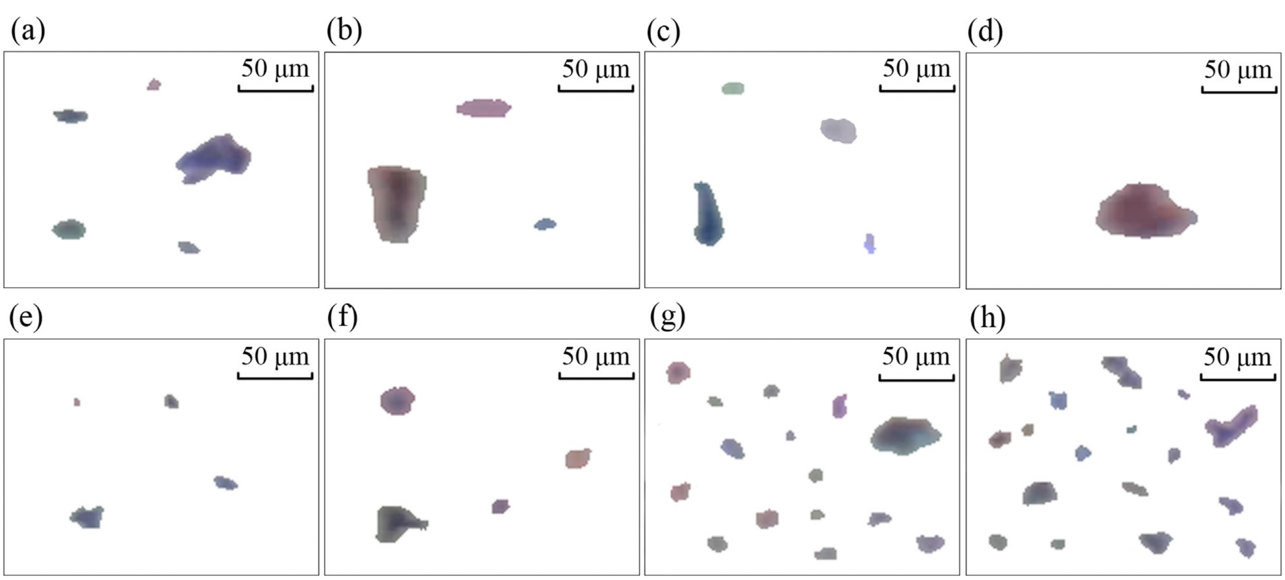

Fig. 2. Eight thumbnail images of wear debris captured in different wear stages: (a) running-in, (b)–(d) normal wear, (e)–(f) severe wear, and (g)–(h) fault.

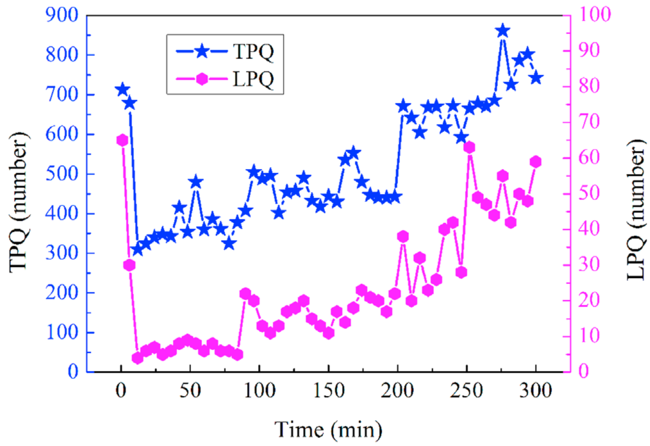

Fig. 3. Variations in the LPQ and TPQ of test #1.

Table 2
Results of the TPQ and LPQ extraction of test #4.

Information	Time of Video Acquisition	
	0 min	6 min
TPQ/number	15847	12361
LPQ/number	512	406

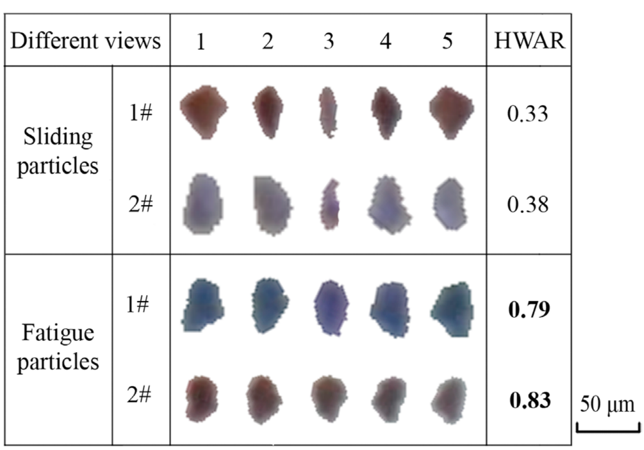

Fig. 4. Multi-view images of two sliding and two fatigue particles as examples.

particles were selected and five different views of each particle are shown in Fig. 4. The HWAR was calculated. Based on the HWAR values, it is easy to distinguish the on-line wear debris. Fatigue particles have higher HWAR values (0.79 and 0.83) than that of sliding particles (0.33 and 0.38). The generation of fatigue debris indicates that fatigue wear of steel balls occurred. Two demonstration videos are uploaded as supplementary materials to show the particles that are in rotational movements, in which the sliding and fatigue particles are easily identified.

From the experimental results in Figs. 2 and 4, it also can be found that the wear particles are in different colours. As mentioned before, the tribo-balls are made up of GCr15. Different colours of the particle materials imply that oxidation wear happened (more colour images can be seen in Fig. 7) by taking reference of our previous work [16]. Therefore, the dynamic features of on-line wear debris, including shape and colour, have been obtained and utilised to achieve a better understanding of the wear conditions.

3.3. Wear state identification

3.3.1. Preliminary wear state identification

As described in Section 3.1, the particle quantity can be used to characterise the changes of wear degree. In order to automatically identify wear states, an intelligent algorithm is employed to establish a model of wear state evolution. Mean-shift is a non-parametric approach for cluster analysis of data samples [27], which is used to classify a series of sample data into different categories. The principle of mean-shift based wear state identification modelling is described below [28].

A set of independent variables are presented by $[x_1, x_2, \ldots, x_n] \in \mathbb{R}$ where n is the number of variables, and are contained in a one-dimensional space. Define an initial spherical space $S_h(x)$ which is centred at x and of radius h. Suppose that there are m samples falling in the same space. The mean distance of all samples can be expressed by a vector $M_h(x)$ which is calculated by

$$M_h(x) = \frac{1}{k} \sum_{x_i \in S_h} (x_i - x), \quad i = 1, 2, \ldots, n. \tag{1}$$

To calculate Eq. (1), a weighted mean is employed. A kernel function $K(x_i - x)$ is introduced to determine the weight of nearby points, and the weighted mean $m(x)$ can be estimated as

$$m(x) = \frac{\sum_{i=1}^{n} K(x_i - x) x_i}{\sum_{i=1}^{n} K(x_i - x)}. \tag{2}$$

Hence,

$$M_h(x) = m_h(x) - x, \tag{3}$$

which is so called mean-shift profile.

The research in [29] indicates that the mean-shift is suitable to model wear state evolution. Therefore, this algorithm is used to cluster the sample data of LPQ into different categories to identify wear status. As Eq. (3) shows, the kernel function $K(x_i - x)$ and radius h are the two basic aspects of mean-shift based wear state identification. There are several kinds of kernel functions are reported, such as uniform function, Cauchy and Gaussian kernels [30–32]. Gaussian kernel is selected to build wear state model because it adapts well to distributed samples [33]. Meanwhile, referring to our previous work [29], the radius is set 0.02. Based on this, the LPQs of tests #1 and #2 are combined together as input, and then a three-step procedure is iterated as follows.

(1) Set the first sampled data to the initial data point x_1. Calculate the weighted mean $m_h(x)$ using Eq. (3).

(2) Set a convergent threshold δ, if $|m_h(x) - X| < \delta$, the procedure is terminated, else repeat step (1).

(3) Update $x_i = m_h(x)$.

After the iterative operation, the samples that share the same centre point are clustered into the same group. The clustering result of the LPQ in Fig. 3 and its corresponding wear state development curve are displayed in Fig. 5. The samples are classified based on their varying gradient and adjacent clusters are marked with different colours. It can be found that the normal wear is divided into three wear states (states 2, 3 and 4), which is consistent to the above description about the material loss of tribo-balls. Although the first two samples are classified into different groups which are marked in red and green colours, they are regarded as the same state (state 1) because they are in a significant fluctuation and very transitory. In the same way, the last three samples in green, blue and black belong to state 5.

Figure 5 shows that an automatic wear state identification model was successfully established using the mean-shift algorithm. This indicates the method of particle counting under dynamic conditions is useful to reveal the changes in the wear rate for wear state

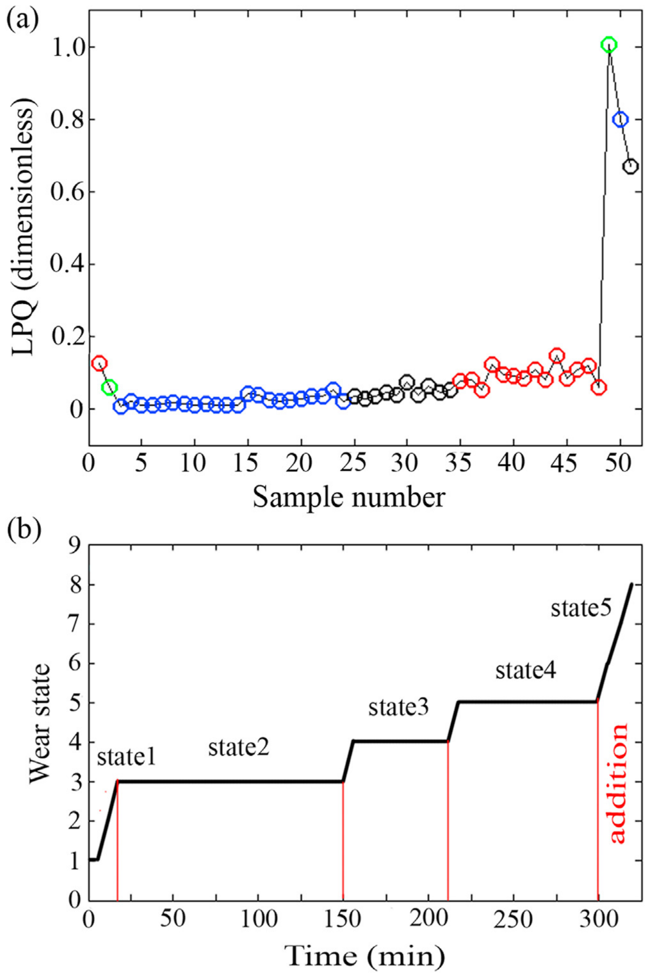

Fig. 5. Results of wear state identification: (a) sample data clustering, and (b) development curve of wear state.

characterisation. However, this model cannot explain that why the wear particles in Fig. 2 various in shape and colours. Therefore, further examination of wear mechanisms is necessary and dynamic features of the wear debris are extracted for this purpose.

3.3.2. In-depth wear state identification

Aiming at in-depth understanding of the wear state evolution, the wear mechanisms were connected with the wear rate to build a new identification model. In this work, statistical features are used to reflect the wear status. The maximum equivalent circle diameter (ECDmax) of each video was extracted and is shown in Fig. 6. Most of the sizes are in the range of [20,40] μm, and the maximum reaches 61 μm. However, only the particles larger than 40 μm can be recognised, as shown in Fig. 6. This is because the on-line wear debris imaging sensor is of low resolution and the particles are in motions.

Correspondingly, the particles marked with numbers were extracted and automatically identified. The results are displayed in Fig. 7. Although some of the particles look similar in shape, such as the particles numbered ①, ②, ③ and ④, their types are different and can be recognised using their multi-view images. As a result, the wear mechanism analysis in a time domain is realised.

By combing Figs. 4 and 7, the wear state transitions of test #1 are comprehensively characterised and shown in Fig. 8. Sliding wear is not indicated in this plot because it is a normal phenomenon and appears in the whole life of a four-ball test rig. From the figure, it can be found that the wear mechanisms are independent

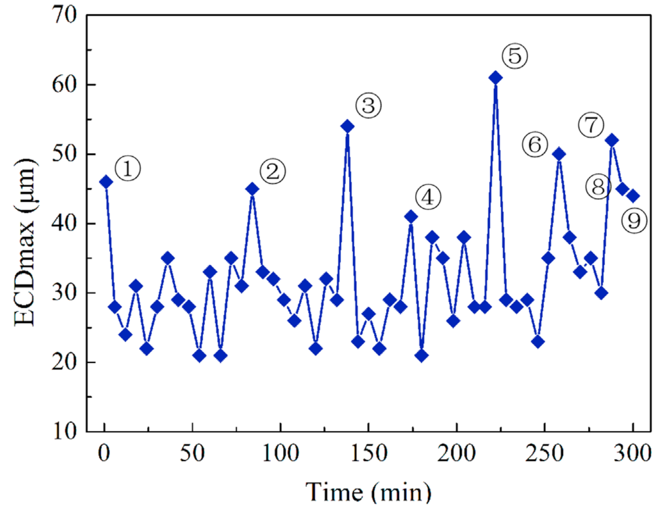

Fig. 6. Variation trend of the wear debris size of test #1.

to the wear rates for the wear state characterisations. Oxidation wear occurred from 139 min onwards. In the last two stages, fatigue wear dominated at 177 min and 295 min but at different wear rates.

3.4. Worn surface examinations of tribo-balls

In order to verify the identification results of the on-line system, the worn surfaces of the tribo-balls in different tests were examined. The wear scars of different tested steel balls are imaged with a microscope and shown in Fig. 9. As shown in Figs. 9(a)–(c), the diameter of wear scar increases with the wear time. Fig. 9(d) is an image of wear crack generated in the destructive test. Although the running time is only 10 minutes, the scar area is larger than that of tests #2 and #3, and the surface is rougher than the others. Furthermore, the wear spots in Fig. 9(c) indicate that not only sliding wear but also fatigue and pitting wear have happened. As described above, the selected tested ball images are representatives of different status identified in one-line analysis. Therefore, the off-line examining results implicitly support that of on-line wear state identification.

4. Discussion

The above analysis results demonstrate that the wear rate and wear mechanism are independent indicators for the wear characterisations. The quantity, shape and colour characteristics of dynamic wear debris are used to examine these two aspects to comprehensively identify the wear status. Compared to our previous work [12] where particle information was used for wear rate assessment, this study enables that more wear information is extracted for wear mechanism examination. Although in this paper the capacity of this development is demonstrated by identifying fatigue and sliding wear as well as oxidation, by extracting more particle features from multi-view images, such as length-to-width ratio and sphericity [15], more wear debris including cutting and sphere particles can be recognised. Therefore, the proposed method can be further developed and applied for wear condition description of other equipment.

Furthermore, there are two aspects need to be mentioned. The first one is that a full-life wear severity examination has not yet performed. The failure progress of this work was simulated by manually changing operating conditions, resulting in a large gap of the particle quantity between tests #1 and #2. Therefore, more

Particle number	①	②	③	④	⑤	⑥	⑦	⑧	⑨
Particle images									
Particle types	sliding	sliding	sliding oxide	fatigue	sliding oxide	sliding oxide	sliding oxide	fatigue oxide	sliding

50 μm

Fig. 7. Identification of the wear debris marked in Fig. 6.

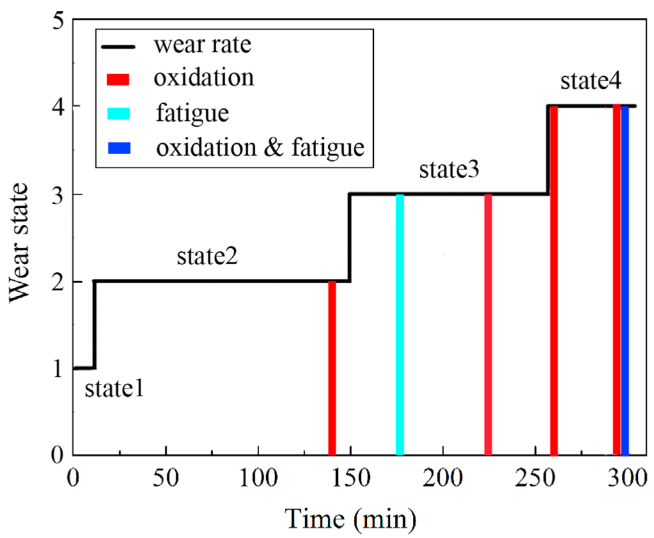

Fig. 8. Comprehensive characterisations of the wear state by combining the wear rate and wear mechanisms.

intensified experiments need to be conducted with various operating conditions to obtain the wear information of the whole lifespan. The intelligent algorithm can be correspondingly developed to make the data clustering more reliable.

The second future area is to improve the accuracy of wear debris recognition. The particles in the range of [20] μm are difficult to be discriminated because of the poor image quality at a low resolution of the sensor. As can be seen in Fig. 9, the mechanism identification is discontinuous from 139 min to 300 min. For the purpose of engineering applications, future work will focus on the optimization design of camera optical systems and the development of image processing and feature extraction techniques to improve the image quality.

5. Conclusions

This paper aims to reveal the wear status of a machine in real time. For this purpose, the wear rate and wear mechanism were both taken into consideration. Comprehensive statistical features including quantity, size, shape and colour were extracted from the dynamic images of moving debris for wear description. Furthermore, intensified and destructive experiments were carried out on a four-ball rig to acquire sample data in different wear conditions to build a full-life identification model. The main conclusions are drawn as follows.

(a) Comparing to the existing on-line monitoring systems, more wear state information was obtained and utilised in the identification model. Wear rate reflected by the particle quantity was used to determine different wear stages. With the time duration, oxidation and fatigue wear occurred and they were examined by the particle shape and colour features.
(b) Large particles (>20 μm contained more wear information than smaller ones (>5 μm). Hence, the LPQ was as the input of wear severity identification modelling with a mean-shift algorithm. The performance of the clustering method was evaluated by examining the post-test tribo-balls.
(c) The HWAR of wear debris was extracted from multiple images at different views. Based on this, fatigue particles were distinguished from sliding debris. Meanwhile, particle colours

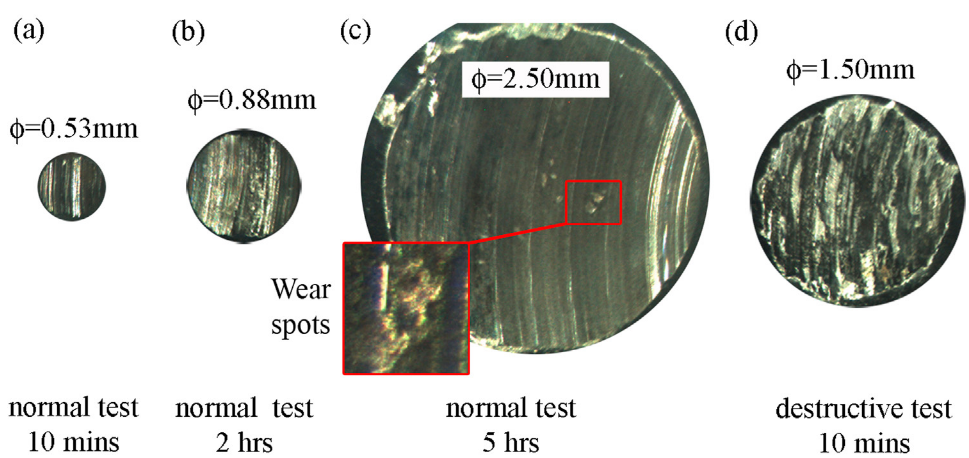

Fig. 9. Wear scar pictures captured from four tests with different running time, (a) 10 min, (b) 2 h, (c) 5 h of the normal tests (tests # 2, 3, 1) and (d) 10 min of the abnormal test (test #4).

were extracted to identify oxidation wear.

(d) Further studies will focus on evaluating the performance of the development by sampling full-life health data, improving image quality for feature extraction of small particles, and developing the reliability of wear state identification algorithm.

Acknowledgements

This work is funded by the National Science Foundation of China (Grant nos. 51675403 and 51275381) and the State Key Laboratory of Mechanical Transmissions of China (Grant no. SKLMT-KFKT-201504).

References

[1] S. Feng, B. Fan, J.H. Mao, Y.B. Xie, Prediction on wear of a spur gearbox by on-line wear debris concentration monitoring, Wear 336–337 (2015) 1–8.
[2] J.Z. Sun, H.F. Zuo, W.B. Wang, M.G. Pecht, Application of a state space modeling technique to system prognostics based on a health index for condition-based maintenance, Mech. Syst. Signal Process. 28 (2012) 585–596.
[3] R. Ahmad, S. Kamaruddin, An overview of time-based and condition-based maintenance in industrial application, Comput. Ind. Eng. 63 (2012) 135–149.
[4] W. Cao, G.N. Dong, W. Chen, J.Y. Wu, Y.B. Xie, Multisensor information integration for online wear condition monitoring of diesel engines, Tribol. Int. 82 (2015) 68–77.
[5] T.H. Wu, H.K. Wu, Y. Du, Z. Peng, Progress and trend of sensor technology for on-line oil monitoring, Sci. Chin. Technol. Sci. 56 (2013) 2914–2926.
[6] Y.Z. Qu, D. He, J. Yoon, B.V. Hecke, E. Bechhoefer, J.D. Zhu, Gearbox tooth cut fault diagnostics using acoustic emission and vibration sensors – a comparative study, Sensors 14 (2014) 1372–1393.
[7] R.C. Liu, H.F. Zuo, J.Z. Sun, L. Wang, Electrostatic monitoring of wind turbine gearbox on oil-lubricated system, Proc. IMechE Part C: J Mech. Eng. Sci. 0 (2016) 1–16.
[8] M. Henneberg, R.L. Eriksen, B. Jørgensen, J. Fich, A quasi-stationary approach to particle concentration and distribution in gear oil for wear mode estimation, Wear 324–325 (2015) 140–146.
[9] P.J. Dempsey, A.A. Afjeh, Integrating oil debris and vibration gear damage detection technologies using fuzzy logic, J. Am. Helicopter Soc. 49 (2004) 109–116 (8).
[10] M. Kumar, P.S. Mukherjee, N.M. Misra, Advancement and current status of wear debris analysis for machine condition monitoring: a review, Ind. Lubr. Tribology 65 (2013) 3–11.
[11] J.Y. Wu, J.H. Mao, W. Cao, Y.B. Xie, Characterization of wear-debris group in on-line visual ferrographic images, Proc. IMechE Part J: J Eng. Tribology 228 (2014) 1298–1307.
[12] T.H. Wu, Y.P. Peng, H.K. Wu, X.G. Zhang, J.Q. Wang, Full-life dynamic identification of wear state based on on-line wear debris image features, Mech. Syst. Signal Process. 42 (2014) 404–414.
[13] T.H. Wu, H.K. Wu, Y. Du, N.M. Kwok, Z. Peng, Imaged wear debris separation for on-line monitoring using gray level and integrated morphological features, Wear 316 (2014) 19–29.
[14] Y.P. Peng, T.H. Wu, S. Wang, N.M. Kwok, Z. Peng, Motion-blurred particle image restoration for on-line wear monitoring, Sensors 15 (2015) 8173–8191.
[15] T.H. Wu, Y.P. Peng, S. Wang, F. Chen, N.M. Kwok, Z. Peng, Morphological feature extraction based on multiview images for wear debris analysis in on-line fluid monitoring, *Tribol. T.* (2017) , http://dx.doi.org/10.1080/10402004.2016.1174325.
[16] Y.P. Peng, T.H. Wu, S. Wang, Z. Peng, Oxidation wear monitoring based on the color extraction of on-line wear debris, Wear 332–333 (2015) 1151–1157.
[17] S. Raadnui, Wear particle analysis-utilization of quantitative computer image analysis: a review, Tribol. Int. 38 (2005) 871–878.
[18] N.K. Myshkin, H. Kong, A.Y. Grigoriev, E.S. Yoon, The use of color in wear debris analysis, Wear 251 (2001) 1218–1226.
[19] J.Q. Wang, L. Zhang, F.X. Lu, X.L. Wang, The segmentation of wear particles in ferrograph images based on an improved ant colony algorithm, Wear 311 (2014) 123–129.
[20] G.P. Stachowiaka, P. Podsiadloa, G.W. Stachowiaka, Shape and texture features in the automated classification of adhesive and abrasive wear particles, Tribol. Lett. 24 (2006) 15–26.
[21] L. Du, J. Zhe, Parallel sensing of metallic wear debris in lubricants using undersampling data processing, Tribol. Int. 53 (2012) 28–34.
[22] M. Ben-Daya, S.O. Duffuaa, A. Raouf, J. Knezevic, D. Ait-Kadi, Handbook of Maintenance Management and Engineering, Springer London (2009).
[23] G.W. Stachowiak, P. Podsiadlo, Towards the development of an automated wear particle classification system, Tribol. Int. 39 (2006) 1615–1623.
[24] C.Q. Yuan, Z. Peng, X.P. Yan, X.C. Zhou, Surface roughness evolutions in sliding wear process, Wear 265 (2008) 341–348.
[25] T.H. Wu, Y.P. Peng, C.X. Shen, J.Y. Wu, Intelligent identification of wear mechanism via on-line ferrograph images, Chin. J. Mech. Eng. 27 (2014) 411–417.
[26] Z. Peng, An integrated intelligence system for wear debris analysis, Wear 252 (2002) 730–743.
[27] V. Miranda, A.R.G. Castro, S. Lima, Diagnosing faults in power transformers with autoassociative neural networks and mean shift, IEEE Trans. Power Deliv. 27 (2012) 1350–1357.
[28] S. Wang, T.H. Wu, H.K. Wu, N.M. Kwok, Modelling wear state evolution using real time wear debris features, *Tribol. T.* (2017) , http://dx.doi.org/10.1080/10402004.2016.1243746.
[29] Y.A. Ghassabeh, On the convergence of the mean shift algorithm in the one-dimensional space, Pattern Recognit. Lett. 34 (2013) 1423–1427.
[30] D. Comaniciu, P. Meer, Mean shift: a robust approach toward feature space analysis, IEEE Trans. Pattern Anal. Mach. Intell. 24 (2002) 603–619.
[31] K.L. Wu, M.S. Yang, Mean shift-based clustering, Pattern Recognit. 40 (2007) 3035–3052.
[32] Y.A. Ghassabeh, A sufficient condition for the convergence of the mean shift algorithm with Gaussian kernel, J. Multivar. Anal. 135 (2015) 1–10.
[33] S.M. Guo, L.C. Chen, J.S.H. Tsai, A boundary method for outlier detection based on support vector domain description, Pattern Recognit. 42 (2009) 77–83.